ARMA 09-155

Statistical Characterization of Rock Structure using LiDAR

Levy, M.E.
SRK Consulting, Denver, Colorado, USA
Visca, P.J.
Independent Consultant, Buffalo Creek, Colorado, USA

This paper was prepared for presentation at Asheville 2009, the 43rd US Rock Mechanics Symposium and 4th U.S.-Canada Rock Mechanics Symposium, held in Asheville, NC June 28th – July 1, 2009.

ABSTRACT: When designing with rock masses of relatively high intact strength, characterization of the geologic structure properties is a critical component to proper analysis. Data describing distributions of discontinuity orientation, length, spacing and strength for pertinent sets within the rock mass provide the basis of probabilistic models necessary for analysis. Probabilistic methods require a reasonably large sample size in order to provide reasonable estimates of inherent structural variability. The use of laser scanning, or LiDAR, technologies is commonly utilized as a high resolution survey technique but is less frequently used, in conjunction with registered high resolution digital imaging, as a tool for geotechnical data collection. This methodology can provide a cost effective and time efficient means of collecting such large data sets. A case study was carried out to evaluate the correlation between statistical characterization of discontinuity properties acquired manually in the field using oriented core and cell mapping techniques to those obtained remotely using LiDAR. The benefits and limitations of these methods are evaluated and practical recommendations are made based on results of the case study.

1. INTRODUCTION

When designing excavations in rock masses of relatively high intact strength, characterization of the geologic structure properties is a critical component to proper analysis. Of the highest order of importance is statistical characterization of discontinuity properties such as orientation, lengths, spacing and strength for pertinent sets within the rock mass. Each of these parameters is best described by a distribution of values having a central tendency and some variation around that central tendency. A sufficiently large sample of the discontinuity population is necessary for development of a representative model.

Several sampling techniques are commonly used for field geotechnical data collection including oriented core drilling and cell mapping. Analysis of orientated core data can reasonably characterize variability in discontinuity orientation, spacing and small-scale joint conditions but information on discontinuity length and large-scale conditions are unattainable from core due to the relatively small sampling window. Manual data collection techniques, such as cell and detail line mapping can yield useful information for characterization of most discontinuity parameters but are commonly restrained by limited safe access to the rock faces and are also frequently time-excessive.

Remote characterization techniques such as LiDAR (Light Detection and Ranging), or laser scanning, are less commonly used but should be considered valid techniques for rapid and accurate geotechnical data collection. LiDAR can provide thorough characterizations of rock structural properties, including discontinuity orientation, spacing and length and, in some cases, large scale roughness or waviness for both surface and underground rock exposures. Compared to manual methods, a large and more accurate data set can be obtained relatively quickly and from a safe distance in areas that would otherwise be inaccessible.

The primary advantage of LiDAR over manual field methods includes the ability to rapidly obtain measurements of rock structure which can be recorded directly into database format during collection. The direct input of the data into electronic format eliminates the time intensive data input steps, and associated sources of error, and greatly simplifies the evaluation of data quality and data management common to most field methods.

The detailed three-dimensional surfaces resulting from the scans also serve as a permanent digital "as-built" record of the excavation, should further examination be desired at a later date, thereby precluding the need for subsequent site visits, in most cases. Sequential scans can also serve as a displacement monitoring system.

The high resolution topographic surveys also provide the accurate information on bench face angles achieved and interramp slope geometries for calibration of backbreak and numerical models. Cross sections or 3-dimensional digital models of geometry and geologic structure can be imported directly into most software packages in dxf format.

It has also been suggested that laser scanning of exposed rock faces can ultimately offer an efficient and rapid method of obtaining probabilistic distributions of block sizes within a rock mass [1].

2. LASER SCAN PRINCIPLES

The laser scan or LiDAR technique is based on the principle that light travels in a straight line and at a constant speed. The LiDAR unit emits a laser pulse and determines the distance to a target based on the time required for the laser to reach the target and reflect back to the unit. Typical LiDAR machines are able to scan from distances up to 1km and at rates of 2,000 to 4,400 points per second creating a three-dimensional data set composed of millions of individual points collectively referred to as a point cloud. Typical accuracy within such point clouds is within several millimeters.

An external software package is typically used to filter the raw point cloud and combine the points into a three-dimensional surface or triangulation irregular network (TIN) by fitting a network of connected triangles to the point cloud.

Data analyzed for this study was obtained using an I-Site 4400CR scanner which automatically integrates linear CCD digital imaging with the three-dimensional laser scan. Together these processes generate a correctly geo-located image-mapped three-dimensional surface from a single point of acquisition [2]. Image calibration automatically performed within the I-Site unit.

3. SOURCES OF SAMPLING BIAS

As with any method of data collection, there are several potential sources of sampling bias associated with laser scanning that should be considered during subsequent analyses. These biases have potential to influence both the quantity and quality of data obtained from the LiDAR scans. Common sources of bias related to sampling technique have been widely documented and are summarized below [3][4][5][6].

<u>Orientation</u> –When perpendicular to the rock surface, discontinuities are only exposed as traces in the rock face instead of a three-dimensional surface making them less visible than those at oblique angles to the face. Discontinuities parallel to the rock face are typically easily detected but underrepresented depending on their spacing. Likewise, observations of discontinuities that are parallel or perpendicular to the laser's line of site can be significantly biased.

<u>Censoring</u> – The extension of one or both ends of a discontinuity beyond the visible exposure can lead to underestimation of discontinuity persistence [5].

<u>Truncation</u> – Discontinuity lengths below a certain size are commonly neglected [5]. This can be particularly common with LiDAR because the generation of the TIN from the point cloud effectively rounds or smoothes the edges and corners of discontinuities to fit them with adjacent data in the triangulation. Truncation bias most significantly impacts data collection for smaller discontinuities.

<u>Length</u> – The probability of sampling persistent discontinuities is greater than the probability of sampling smaller ones [3]. In addition, joints are likely more persistent than suggested by the exposed or visible plane. This concept of "exposed persistence" suggests that the exposed discontinuity surfaces represent the minimum persistence, or lower bound average persistence for each discontinuity set [6].

<u>Occlusion</u> – Certain portions of the rock mass are obscured by other portions and the information contained in these hidden areas will be omitted from the point cloud. Data occlusion caused by the line of site from one location can only be corrected by scanning the rock mass from another location or direction and combining the results. To minimize the impact of occlusion, sampling should be undertaken on different outcrop faces at varied orientations in three dimensional space [7].

4. CASE STUDY BACKGROUND

A case study was carried out to evaluate the correlation between the statistical characterization of discontinuity properties acquired manually in the field with oriented core and cell mapping to those obtained remotely using LiDAR scanning. The subject site for the study is an open pit mine excavated in a competent granodiorite rock mass where typical instabilities are related to geologic structure.

Field discontinuity characterization of core was conducted by orienting discontinuities from approximately 625m of core from four different drill holes. Holes drilled with inclinations toward the north, south and west were selected to provide a relatively unbiased data set for comparison with the LiDAR data. A total of 894 discontinuities were oriented in the four holes using the Reflex A.C.T. system [8].

Core logging procedures included measuring discontinuity orientation (dip and dip direction) and noting small and intermediate-scale roughness and infillings. The core orientation, geotechnical logging and data analysis is estimated to have taken approximately 30 days to complete.

Exposed and accessible bench faces were mapped using the cell mapping technique. A total of 135 discontinuity measurements were taken over 26 cells encompassing a linear distance of approximately 820m. Discontinuity properties recorded during cell mapping included discontinuity orientation, length, spacing, large-scale roughness, infillings and terminations. The cell mapping program and data analysis took approximately six days to complete.

Pit walls in the same area were surveyed from five different locations using an I-Site 4400CR laser scanner automatically integrating a high resolution panoramic digital image with the three-dimensional point cloud. The total area scanned is approximately 600m in length, 100m in height and included four mining bench levels. The scanning and data processing required less than one day to complete. Approximately two additional days were necessary to digitize the discontinuities and analyze the data.

After filtering the initial point cloud, a TIN was generated with the high resolution image registered and "draped" over it forming a detailed three-dimensional digital surface for analysis. Simple digital enhancements such as lighting can be performed on the images prior to or during analysis for situations where relatively poor weather or lighting conditions exist at the time of scanning. In addition, any number of lighting combinations can be made within most 3D modeling packages to illuminate the TIN surface simulating different sun light angles often viewed as important vantage points in field geology.

All visible discontinuities on the surfaces were digitized using the Vulcan Geotechnical Module which automatically inputs the structural data directly into an exportable database file [9]. An example of a typical 3-dimensional digital bench face model is shown on Figure 1 with the digitized structures colored by joint set.

The parameters that were automatically collected in the geotechnical database for each discontinuity digitized included discontinuity type, coordinates (easting, northing and elevation), orientation (dip and dip direction), length, spacing and termination (single, double or none). Vulcan allows the database to be modified to contain nearly any additional parameters or combination of parameters desired by the user.

The Vulcan Geotechnical Module has a built-in stereonet window to facilitate visualization and analysis of the discontinuity orientation data collected. Each discontinuity digitized on the 3-dimensional model (Figure 1) is linked directly to the stereonet through the geotechnical database. This allows the user to evaluate the 3-dimensional location(s) of certain discontinuities or sets of discontinuities within the rock mass or, conversely, to evaluate stereoplots of discontinuities contained in discrete areas of the rock face.

By digitizing each structure, more subjective judgment of the user is allowed, limiting the potential for erroneous data that can sometimes result from automated methods of analysis.

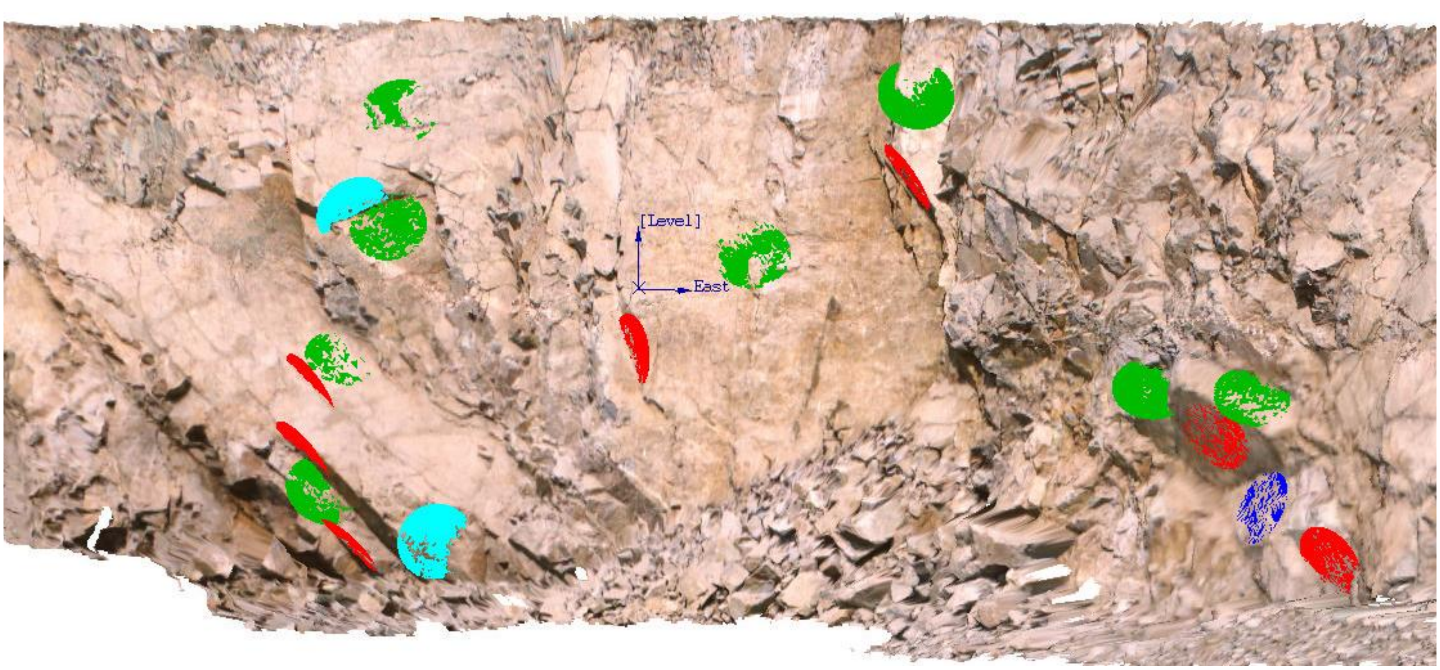

Fig. 1. Typical 3-dimensional bench face model obtained remotely using LiDAR. Digitized structures are shown as discs colored by joint set.

Lower hemisphere, equal area stereoplots were prepared for each of the three sampling techniques for visual comparison and are presented in Figure 2 through Figure 5.

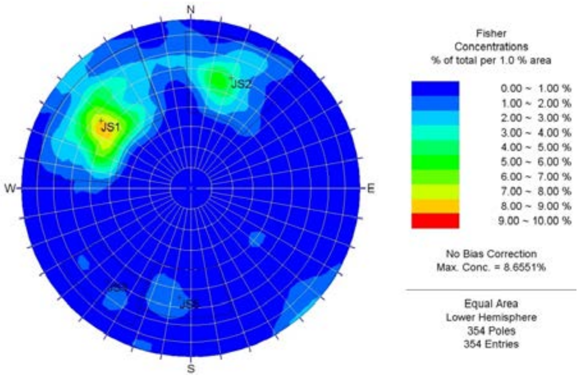

Fig. 2. Stereoplot of discontinuities obtained with LiDAR.

The LiDAR scans were conducted from central locations in the pit, scanning toward directions of approximately 090 to 220 degrees azimuth.

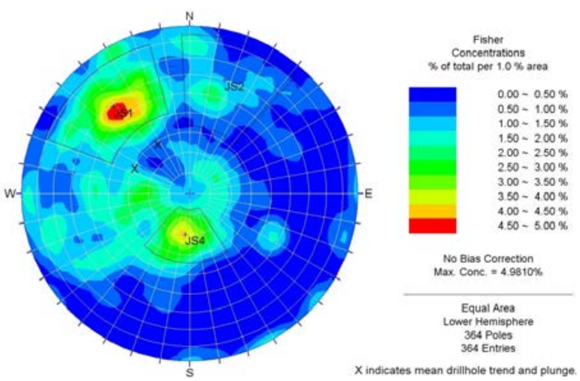

Fig. 3. Stereoplot of oriented core discontinuities from two drillholes drilled with inclinations towards the northwest.

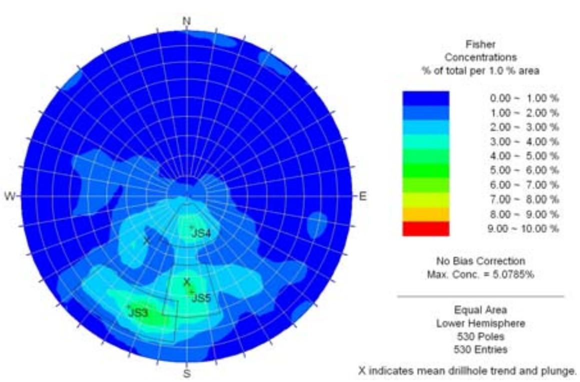

Fig. 4. Stereoplot of oriented core discontinuities from two holes drilled with inclinations towards the south and southwest.

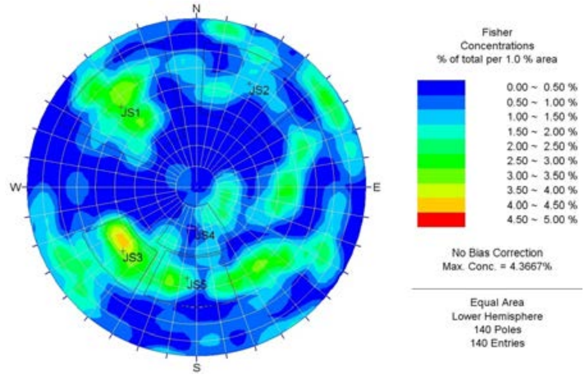

Fig. 5. Stereoplot of discontinuities obtained by cell mapping.

Visual inspection of the plots revealed up to five common joint sets between the different sampling techniques. The mean and standard deviation of orientation properties for each set are summarized in Table 1 for each of the sampling techniques.

Table 1. Summary of joint set orientation statistics

Set ID	Sampling Method	No. of Samples	Dip Angle (deg)		Dip Dir. (deg)	
			Mean	**Stdev.**	**Mean**	**Stdev.**
J1	LiDAR	148	**56**	11.2	**127**	15.7
	Core (199m)	86	**58**	10.5	**139**	13.9
	Cell Mapping	24	**55**	13.2	**137**	12.6
J2	LiDAR	68	**59**	11.7	**200**	11.5
	Core (199m)	37	**60**	13.0	**197**	13.7
	Cell Mapping	8	**58**	8.8	**208**	13.4
J3	LiDAR	12	**63**	6.5	**42**	12.8
	Core (424m)	80	**64**	5.8	**28**	12.6
	Cell Mapping	14	**48**	6.6	**49**	10.2
J5	LiDAR	17	**55**	3.8	**6**	12.5
	Core (424m)	51	**48**	8.1	**358**	7.0
	Cell Mapping	11	**45**	6.5	**6**	16.6
J4	LiDAR	Set J4 is not apparent from the LiDAR data				
	Core (625m)	72	**18**	6.1	**1**	21.5
	Cell Mapping	6	**20**	8.4	**2**	27.5

Attempts to identify and compare "best-fit" statistical distribution types for dip and dip direction were also compared for each data set; however, due to lack of data for some data sets, a reasonable comparison was not able to be made.

Distributions of discontinuity lengths were, however, able to be compared for the cell mapping and LiDAR data sets. As previously discussed, measurements of discontinuity length were digitized directly from the LiDAR scans providing an exposed length for each of the 354 discontinuities digitized. The frequency and distribution of discontinuity lengths digitized using the LiDAR derived models are presented in Figure 6.

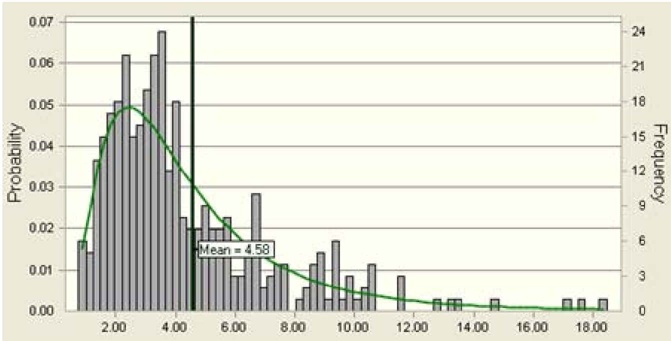

Fig. 6. Distribution of discontinuity lengths obtained from LiDAR scans.

Figure 6 represents the overall distribution of lengths of discontinuities from all sets combined. If desired, a separate distribution of lengths could just as easily be obtained for each of the five discontinuity sets.

Estimates of discontinuity length were made as part of the field cell mapping sampling program; however, only set maximum lengths were estimated to keep the program within reasonable time constraints. The distribution and frequency of discontinuity length estimates obtained by cell mapping are presented in Figure 7.

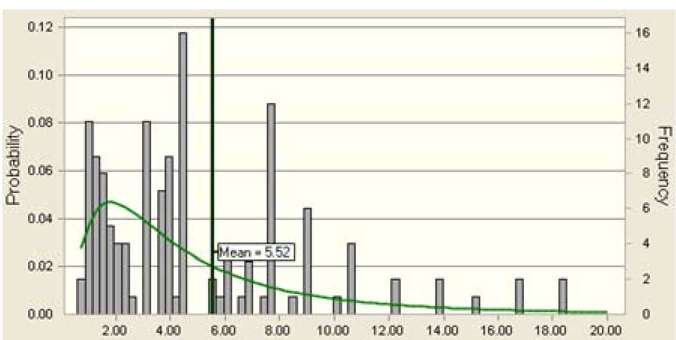

Fig.7. Distribution of discontinuity lengths obtained with field cell mapping.

It is apparent from Figure 7 that relatively limited data was obtained from cell mapping, lowering the confidence in the distribution compared to the LiDAR derived distribution shown in Figure 6. Another limitation of the cell mapping sampling technique, compared to LiDAR, is that the length measurements are mere estimates made in the field from distant and often less than ideal vantage points.

The LiDAR distribution of discontinuity lengths may be somewhat biased on the short side due to digitizing of their "exposed persistence" as previously discussed. The cell mapping technique can offer the advantage of being able to better estimate what portion of the discontinuity is exposed.

As would be expected, no information regarding discontinuity length was available from the oriented core discontinuity sampling.

Following the initial comparison of the discontinuity plots and statistics, the data sets were evaluated for potential sources of bias to determine what impacts biases may have had on the results of each sampling technique.

5. DISCUSSION

From the stereoplots and discontinuity statistics, it is evident that the two most prominent joint sets, J1 and J2, are adequately sampled and characterized by each of the field and LiDAR sampling techniques. Such frequent sampling of J1 and J2 with the LiDAR may not have been initially suspected since the sets nearly parallel the outcrop faces. However, visual observations of the rock mass indicate plane-shear type features are common from these sets which provide good reflective surfaces for LiDAR.

Reasonably good correlation is also noted between the core and LiDAR data sets for J3 and J5; however, the cell mapping data tends to reflect a lower mean dip angle than the core and laser scan data. This could be a result of field estimation accuracy or due to the lack of data points in the cell mapping data set.

The two field sampling methods show good correlation for joint set J4; however, this set is not apparent in the LiDAR data set. The absence of J4 is likely a direct result of an orientation bias because it is oriented nearly perpendicular to the outcrop face and parallel to the LiDAR line of site causing members of the set to be masked as sub-horizontal cracks or traces in the rock face. In addition, the orientation of set J4 is such (shallow dip into the wall) that it is unlikely that either backbreak or structural displacements would involve this set leaving relatively few members of J4 actually exposed for laser reflection.

Although some indication of sets J3 and J5 is evident in the LiDAR data set, they also appear to have been under sampled compared to sets J1 and J2. Joint sets J3 and J5 also strike sub-parallel to the exposure but have a steeper dip angle than set J4. The steeper dip angles may have resulted in more J3 and J5 surfaces being exposed as back releases for inward dipping J1 and J2 structural displacements. The addition of another scan location at a higher elevation or from a more oblique angle would likely yield more frequent sampling of sets J3, J4 and J5.

From the comparison, it is evident that an orientation bias does occur when discontinuities are oriented perpendicular to the outcrop face or sub-parallel to the laser's line of site. Discontinuities such as these are particularly difficult to detect for automated types of analyses but by digitizing with the use of a high resolution image properly registered and "draped" over the TIN, orientation biased discontinuities can be digitized, particularly if three or more points can be located on the surface with sufficient relief.

Distributions of discontinuity lengths were also statistically evaluated for the cell mapping and LiDAR sampling techniques. While the LiDAR sampling method provided a larger data set and higher level of confidence, the cell mapping also yielded similar statistical parameters. The mathematical “best-fit” to both data sets was determined to be a lognormal distribution with mean values of 4.6m and 5.5m for the LiDAR and cell mapping data, respectively. The LiDAR distribution is likely affected to some extent by length bias, measuring the “exposed persistence” for some discontinuities yielding a slightly lower estimated mean length. However, considering inaccuracies associated with all measurements of discontinuity length or persistence, the mean values and distributions obtained are considered quite similar for both methods.

In addition, it is worthy of noting that the smallest discontinuities recorded were 0.75m and 0.61m for the LiDAR and cell mapping techniques, respectively. The frequency of both distributions begins to taper off below a length of about a 2m to 3m indicating that shorter length discontinuities were probably under sampled compared to longer length discontinuities. This is likely the product of a truncation bias considering discontinuity length is typically best described by a negative exponential distribution indicating the shorter the discontinuity length, the higher the frequency of occurrence. However, characterizations of longer lengths are typically of primary interest for design analyses as smaller length discontinuities typically have a less significant impact on design.

Discontinuity set spacing distributions can also be estimated from LiDAR data by using a “virtual scan line” technique [6]. This method involves using a line normal to the mean discontinuity set orientation and either counting the number of intersections between members of the set and the line or by measuring the individual distances between discontinuities along the line. The number of discontinuity intersections with the “virtual scan line” divided by the length of the line (i.e. the mean spacing) can be used to describe a negative exponential distribution to adequately characterize discontinuity spacing. True spacing can also be calculated with this method using the unit vector and length of the scan line. Some judgment is necessary to select where to insert the “virtual scan line” or lines into the model.

Measurements of true and apparent spacing can be digitized directly into the Vulcan database where the spacing between discontinuities is visible. The ability to adequately capture discontinuity spacing with LiDAR is dependent on the orientation of the scan relative to the orientation of the set(s) and the spacing distances themselves.

Censoring bias appears to have had an insignificant impact on the LiDAR data sets since the scans and images were able to cover relatively large areal expanses in this particular case. Having the high resolution image accurately registered to the TIN also allowed better identification of discontinuity termination and evaluation of the extents of their characterization.

Several relatively small areas of occlusion were noted during the analysis of the LiDAR data. In most cases, alternate scans were able to be analyzed when areas of occlusion were identified in a particular scan. Very rarely did more than one scan occlude the same area. It was noted that the closer the outcrop was to paralleling the scanner line of site, the higher the frequency of occluded areas. More careful planning of the scan set-up locations and elevations would have helped reduce the areas of occlusion; however, it is highly unlikely that a complete scan of any outcrop could be obtained without occlusion of at least some areas.

6. CONCLUSION

A case study was carried out to evaluate the correlation between statistical characterization of discontinuity properties acquired manually in the field using oriented core and cell mapping techniques to those obtained remotely using LiDAR. Results of each sampling technique were plotted on stereonets for visual comparison and statistical parameters were calculated for direct comparison of the data sets. The comparison of the LiDAR derived discontinuity sets with the field measurements verified that LiDAR can provide an accurate assessment of rock structure. The good correlation between the LiDAR and field methods also validates the use of non-automated techniques of remote discontinuity data collection.

Oriented core can provide a thorough sample and distribution of orientation data but is unable to yield information regarding discontinuity length or large scale roughness. Oriented core drilling is also a much more time intensive and expensive program than LiDAR if structural characterization is of primary interest. In some cases, however, outcrops of sufficient size and condition to support LiDAR scanning are not exposed during feasibility and design level investigations, restricting its use.

The greatest advantage of LiDAR over manual field sampling techniques is its ability to acquire comparatively large and accurate data sets, including discontinuity orientation, length and spacing, in a relatively small time frame and with very limited personnel exposure in areas that may otherwise be unsafe and inaccessible. With the relatively large data sets collected using LiDAR scans, statistical distributions can easily and confidently be evaluated as opposed to "best guesses" based on the relatively few data points typically obtained from manual field mapping.

Using 3-dimensional mine planning software such as the Vulcan Geotechnical Module for analysis of the scan allows direct input of the various structural parameters into an electronic database format that can be easily exported into other analysis packages. The direct input of the data into electronic format eliminates the time intensive data input steps, and associated sources of error, and greatly simplifies the evaluation of data quality and data management common to most field methods. For this case study, the LiDAR scanning and data post-processing as well as the discontinuity digitizing and data analyses were all completed in less than three days.

The LiDAR technique is susceptible to different sources of bias as are field sampling techniques. However, with a carefully designed, well thought out plan, the potential for sampling bias can be minimized. The plan should include scanning of the same outcrops from multiple angles or locations to reduce areas of occlusion and to provide optimum coverage and overlap in areas of primary interest.

Digitizing of discontinuities from LiDAR data requires good geotechnical engineering judgment when selecting and measuring relevant discontinuity surfaces. However, even with good judgment, it is very difficult to characterize the discontinuity conditions such as small-scale roughness and infilling with remote techniques. Remote methods cannot replace important field observations such as rock hardness and weathering conditions of discontinuities, although with the combination of the scan and high resolution image, reasonable estimations can be made if the user is familiar with site conditions from prior site visits.

Structural characterizations based on LiDAR scanning should ultimately be confirmed with some level of field reconnaissance to verify data gaps characteristic of known biases. Above all, remote methods should be considered to be a useful and efficient way to provide objective rock mass information which can be used to supplement the subjective observations and assessments of the geotechnical engineer.

REFERENCES

1. Turner, A.K., J. Kemeny, S. Slob and R. Hack. 2006. Evaluation and management of unstable rock slopes by 3-D laser scanning. In *10th Congress of the International Association of Engineering Geology and the Environment, London, 18-21 September 2006*.
2. Ratcliffe, S. and A. Myers. 2006. Laser Scanning in the Open Pit Mining Environment – A Comparison with Photogrammetry. I-Site Product Development White Paper.
3. Sturzenegger, M., M. Yan, D. Stead, and D. Elmo. Application and limitations of ground-based laser scanning in rock slope characterization. In *Proceedings of the first Canadian US rock mechanics symposium, vol. 1., Vancouver, 27-31 May 2007*, eds. Eberhardt, E. D. Stead and T. Morrison, 29-36. London: Taylor & Francis.
4. Terzaghi, R.D. 1965. Sources of error in joint surveys. *Geotechnique*. 15(3): 287-304.
5. Zhang, L. and H.H. Einstein. 1998. Estimating the mean trace length of rock discontinuities. *Rock Mechanics and Rock Engineering*. 31(4): 217-235.
6. Strouth, A. and E. Eberhardt. The use of LiDAR to overcome rock slope hazard data collection challenges at Afternoon Creek Washington. In: *Proceedings of the 41st US Symposium on Rock Mechanics, Golden, 17-21 June 2006*, eds. D. Yale, S. Holtz, C. Breeds and U. Ozbay.
7. Priest S.D. 1993. *Discontinuity Analysis for Rock Engineering*. 1st ed. London: Chapman and Hall.
8. *Advanced Core Orientation Tool*, Reflex Instruments, Ontario, Canada.
9. *Vulcan 7.5.627*, Maptek Pty. Ltd., Lakewood, Colorado. 2009.